International Journal of Aeronautical and Space Sciences, Volume 24, Issue 3, July 2023, pp. 812-823
DOI: 10.1007/s42405-022-00559-z

Dynamic Simulation and Aircraft Level Assessment of CMC Implementation on GTF Engine

Da Mo[1]

Centre for Propulsion Engineering, School of Aerospace, Transport and Manufacturing, Cranfield University, Bedfordshire, MK43 0AL, United Kingdom

AECC Shenyang Engine Research Institute, Shenyang, 110015, China

Ioannis Roumeliotis[2]

Centre for Propulsion Engineering, School of Aerospace, Transport and Manufacturing, Cranfield University, Bedfordshire, MK43 0AL, United Kingdom

Yixiong Liu[3]

Centre for Propulsion Engineering, School of Aerospace, Transport and Manufacturing, Cranfield University, Bedfordshire, MK43 0AL, United Kingdom

AECC Shenyang Engine Research Institute, Shenyang, 110015, China

Christos Mourouzidis[4]

Centre for Propulsion Engineering, School of Aerospace, Transport and Manufacturing, Cranfield University, Bedfordshire, MK43 0AL, United Kingdom

Sajal Kissoon[5]

Centre for Propulsion Engineering, School of Aerospace, Transport and Manufacturing, Cranfield University, Bedfordshire, MK43 0AL, United Kingdom

Abstract

This paper dynamically simulated the geared turbofan engine with CMC turbine components, including impacts of fuel schedule, shaft inertia, volume packing, BOV schedule. Deliberated

[1] Senior Engineer, Corresponding author: dada1204@126.com
[2] Senior Lecturer.
[3] Senior Engineer.
[4] Lecturer.
[5] Research Fellow.

comparisons were performed between CMC engine and Inconel engine on aircraft level performance and transient behaviour. Heat load examination is included in flight mission analysis, which lays the basis on the gearbox efficiency map related to torque and rotational speed. Results indicate that IPC surge margin of the CMC case slightly fall 0.15% but maintain steady. The mitigated T4 overshooting phenomenon has offered a 30K drop and thus extended turbine life. More importantly, Fan shaft inertia dominantly affects engine operability whereas the blow-off air fraction severely impacts the low power setting operation. Further investigation of heat load reveals that power loss at take-off segment accounts for 1.1% of IP shaft input power, which is 3.98% higher than Inconel case. The thermal management system needs to be redesigned to absorb extra heat. On assessment of aircraft level performance, CMC engine provides superior profits in maximizing airline revenue. The predicted annual fuel cost saving is about 0.08 million dollars coming from block fuel reduction. NOx, noise and CO2 demonstrate obvious decline, approaching 5.9%, 1.0% and 4.9% respectively.

Key words: CMC; aircraft level performance; transient performance; heat load; emissions

1. Introduction

The raised taxes, airport usage fees, and cheap airfare have tremendously suppressed airline revenue. Moreover, the growing fuel price and stringent environmental guideline have constrained the development of conventional turbofan engines with relatively high fuel burn, noise and emissions. The fuel consumption growth is devastating because of the rising cost and environmental concerns. The noise mainly comes from the high fan tip speed and bothers the residents nearby the airport. The above problems have motivated designers to develop more eco-friendly and fuel-efficient engines. Therefore, improvement in specific fuel consumption (SFC) improvement and engine weight is a necessity, which could be mainly addressed by increasing components efficiency, thermal efficiency and propulsive efficiency. To be specific, according to Dewanji [1], higher BPR and OPR could improve performance, while lower fan tip speed and LPT stage counts could lessen noise and engine weight. Based on the conventional turbofan, geared turbofan (GTF) engine configuration is established by fitting with a power gearbox (PGB). Larsson [2] found that PGB may apparently cut

engine weight, minimizing the low pressure turbine (LPT) stage numbers and shaft weight of the low pressure (LP) system. The introduced PGB could isolate the Fan from the LP system and differentiate their speed. Thus, LPT could rotate at high speed with satisfactory work output, while Fan spins slowly with less noise. GTF engine is recommended in relation to the following advantageous aspects:

1. Higher BPR and lower FPR.
2. Decreased fan tip speed and lower noise emission.
3. Lighter engine weight.
4. Reduced specific fuel consumption, fuel burn and carbon dioxide emissions.

Nevertheless, a well-designed engine should not only have superb aerothermal performance but could also function properly. Aircraft engines frequently encounter compressor aerodynamic instability issues ([3][4][5]), especially in the start-up, shut down or part power operations. Fan and IPC are prone to surge at low corrected speed due to the large incidence angle, leading to flow reversal, blade vibration, flame-out and even blade failure[3]. Effective measures could be taken to tackle the possible risks. Blow-off valve (BOV) and variable area nozzle (VAN) will switch the running line away from the surge line without altering the engine configuration. Variable stator vane (VSV) and variable inlet guide vane (VIGV), on the other hand, adjust the compressor inlet area to increase the surge margin. Mourouzidis [6] implemented the adoptions of the variable area fan nozzle (VAFN) during the engine cycle design in order to improve fan performance and operability. Other studies looked into the effects of the potential strategies described above. Woodward [7] tested the impact of VAFN area in a wind tunnel at sea level condition and concluded that the noise could be effectively decreased by more than 2dB with the 5.4% enlarged VAFN area. Halliwell [8] explored the benefits of variable pitch Fan (VPF) on fuel consumption and found that the engine with VPF consumed 3.8% more mission fuel due to the increased ram drag during the cruise segment. But the VPF still showed great potential in enhancing propulsive efficiency.

Although the strategies presented above could prevent the engine from surge, it is crucial to examine the transient behaviour and performance to ensure the engine operates properly under the given control system. The engine seldom works in a steady-state (SS) situation and frequently

experiences transient operation like sudden throttle pulling. Slam acceleration and deceleration often cause a noticeable shift in the compressor operating line and endanger the engine operation. Besides, the impacts of the deployed gearbox should also be taken into account when the GTF engine operates in a transient process. Much heat rejection coming from friction would be generated in the PGB system and produce unacceptable power losses [9]. This amount of power losses would also affect engine performance [10]. Consequently, effective lubrication and cooling system are highly demanded to preserve the performance and life span of PGB [9]. Manuel [11] discovered that temperature and the power dissipation of PGB and transient behaviour are mutually influenced. Therefore, it is of great significance to investigate the heat load of the GTF during transient operation.

Numerous studies have assessed the engine transient behaviour and performance. Wang [12] utilized Turbomatch software to inspect the transient performance of the clean and degraded engine. The distinguishing impacts of the turbine and compressor depletion were discussed. The comparisons uncovered that the turbines degradation effects are much more severe than those from compressors. Zhang [13] launched the engine model and control system with the assistance of Gasturb and Matlab/Simulink. The acceleration process from idle to 105% speed was compared with idle to 120% speed, finding that the protection measure could protect the fuel from overfueling. Roumeliotis [14] first built a hybrid model for helicopter engine in Simcenter Amesim and studied the transient performance differences between the simple cycle and recuperated cycle. The results revealed that the transient response of the recuperated engine lagged almost 10s to achieve the steady state compared to the simple cycle.

There are some manoeuvre concerns regarding transient behaviour, such as fuel profile, shaft inertia, BOV schedule and volume packing. For fuel pumped periods, Yang [15] compared the transient responses with 0.05s, 1s, 2s and 4s, observing that a slam acceleration would be inclined to induce surge issue. The mechanical system acts slower than aerodynamic system because of the shaft inertia delay. Wang [12] conducted a dynamic simulation with the original IP shaft inertia and cut-half inertia. IPC working line is found to be closer to SS line with smaller inertia. The variation of the air mass flow might eventually alter the engine dynamic performance. The volume packing effects were also

investigated using the intercomponent volume (ICV) method.

Another point worth mentioning is that ceramic matrix composites (CMC) implementation has significantly improved engine performance and reduced engine weight. Actually, the implementation of CMC on gas turbine engine are not uncommon. For example, two types of CMCs exhaust nozzle were investigated with regard to the durability and suitability. It was found that the delaminations induced by the acoustic loading and thermal gradient were severe, especially at the connection areas with metallic components [16][17]. Also, CMCs seal was also investigated and the seals experienced 11161 tactical air cycles[18]. The CMCs material used for turbine component were also studied by many researchers [19][20]. Langenbrunner [21] examined the tip rub for a CMC and metal turbine blade and claimed similar abilities concerning the rub event. However, there still exist some disadvantages and challenges for CMC turbines. The constitutive model of CMC is still not well explained and the failure mode is not accurately predicted. Meanwhile, the dispersion of the mechanical properties of CMC material is still a critical issue for engineering practice. More importantly, due to the anisotropic characteristics, conduction coefficient alteration and strength difference between CMC and the base, design of hot component CMC is a huge challenge. To date, few studies have investigated the dynamic response on the engine deploying CMC.

This paper is a continuous work of Mo [22] and the findings will generate fresh insight into how the CMC turbine application would impact transient performance of GTF engine. It aims to further explore the area of CMC implementation on GTF engine transient response and flight performance. The GTF engine with Inconel 718 turbine was set as baseline powering A320-type aircraft. The simulation was carried out in Simcenter Amesim 2020.1 edition [23] which is commonly used in aeronautics domain. Key issues concerning engine operations, fuel, BOV schedule, volume packing, shaft inertia and PGB thermal load are covered. Sensitivity analysis regarding effects of the above factors is performed to identify the predominant element on engine dynamic performance. Meanwhile, aircraft-level flight mission is assessed to seek the advantages of CMC turbine.

2. Methodology

The steady-state parameters of the Inconel718 and CMC cases are compared in Table 1. The BPR

for CMC case has risen to 15.51, 17.95% larger than the Inconel case. The primary reason for that is the distinct reduction in cooling air demand since the CMC features a higher blade metal temperature. The saved cooling air would generate augmented core thrust. Consequently, more air has to be driven into the bypass passage to maintain the same required thrust level.

Table 1 Parameters comparison

Material	Inconel 718	CMC
Dfan(m)	1.9	1.9
BPR at CR	13.15	15.51
OPR at CR	60	60
T4 at TO(K)	1950.0	1950.5
Cooling air fraction (HPT&NGV)	15%	0.16%
FN at TO(kN)	120	120
Engine weight(kg)	1735	1687
SFC at CR((g/s)/kN)	12.64	12.16

2.1 Transient Model Establishment

In the newly launched Amesim 2020.1 [23], the design point could be evaluated using the embedded Gas Turbine Performance tool. The static architecture would be generated automatically after the basic parameters are input, presented in Fig. 1. Concerning the component maps, the default maps in Amesim would be scaled based on the established engine configuration.

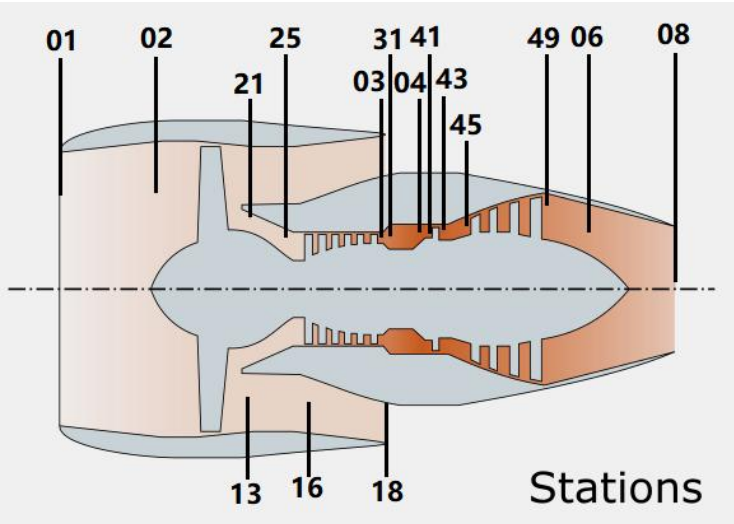

Fig. 1 A two-shaft turbofan engine architecture.

The developed transient model for the GTF engine with CMC turbine is established and shown in

Fig. 2. The transient model comprises of core fan, bypass fan, HPC, IPC, HPT, LPT, burner, nozzles, shafts and gearbox. It should be noted that the HPT, IPT and LPT blades and vanes were assumed to be manufactured with CMC material. The SiC/SiC CMC was implemented with blade metal temperature reaching 1755K [24].

Specific modules such as BOV, flight Mission, and fuel controller and heat load module are introduced. BOV is placed at the last stage of IPC to blast off the excessive air at low corrected speed. The flight mission module covers various flight environments by entering the Mach number and altitude. In addition, several transmitter and receiver sensors are coupled to transmit the total and static aerodynamic properties. When performing flight mission simulation, PID controller module and emission estimation module is activated. PGB heat load is estimated using the reducer heat losses module.

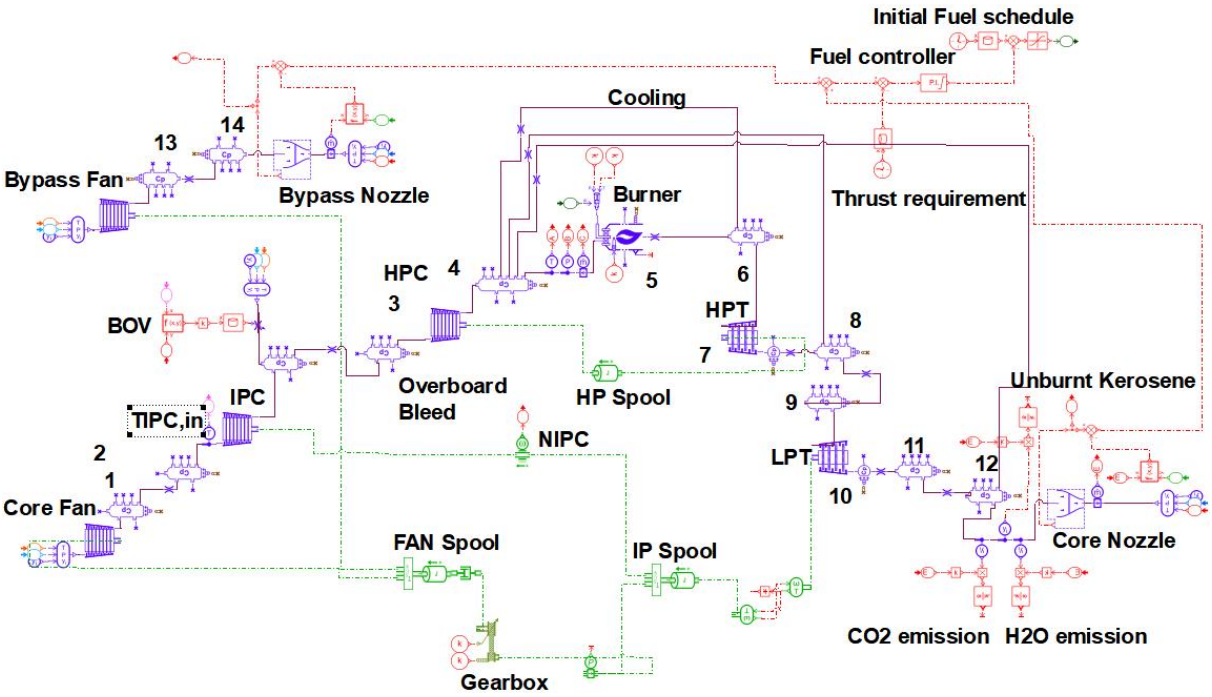

Fig. 2 Geared turbofan engine transient model.

2.2 Investigation Method

2.2.1 Fuel Schedule

The fuel regulation explicitly specifies the engine power settings. The shaft speed would be boosted when extra fuel is pumped into the combustor, and the acceleration is activated. As mentioned above, fuel flow control exerts a significant influence on transient behavior. Typically, a gas turbine engine is

supposed to accelerate within 8 seconds on slow acceleration conditions [4]. In this study, the duration of 4s, 6s and 8s for acceleration and deceleration were investigated in order to figure out the influences of slam acceleration or deceleration. The scheduled fuel profile is presented in Fig. 3. with fuel flow reaching 0.4kg/s and 0.76kg/s in idle and take-off segments.

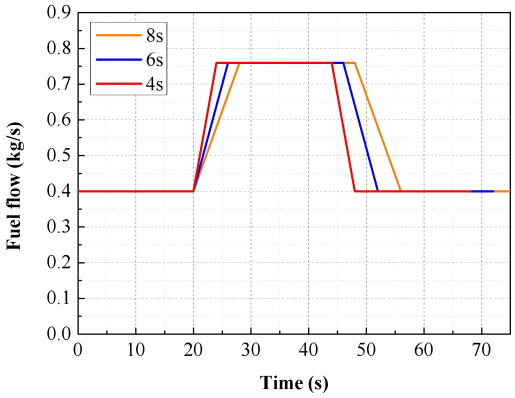

Fig. 3 Fuel schedule for acceleration and deceleration.

Shaft inertia always delays the shaft speed response when there is a rapid fuel change. It is essential to recognize the degree to which the engine operability is related to the shaft inertia. The moment inertia was calculated according to Equation (1)[25]. Radius and component rotating mass, which includes the mass of blades, disks, and shafts, are the two critical parameters that influence inertia. The calculated shaft inertia of the geared turbofan engine is listed in Table 2. The moment inertia for HP and LP systems have considered the application of CMC material for HPT and LPT blades and vanes.

Reaching almost seventeen times the IP shaft inertia, the Fan shaft inertia ranks top whereas the HP shaft inertia senses the bottom. Seven cases were established to study the effects of shaft inertia on engine performance, as presented in Table 3. The cases were established to examine the impact of shaft inertia on the engine transient behaviour by scaling the inertia values.

$$J = \frac{1}{2} m_R (R_0^2 + R_i^2) \tag{1}$$

Where

J is the moment inertia (kgm^2).

m_R is the rotating mass (kg).

Ro is the outer radius (m).

Ri is the inner radius (m).

Table 2 Shaft inertia of GTF engine with CMC turbines

Shaft	Component	Ri (m)	Ro (m)	m_R (kg)	J (kgm^2)	J_{Total} (kgm^2)
HP	HPC	0.056	0.129	22.43	0.222	0.38
	HPT(CMC blades&vanes)	0.056	0.156	10.11	0.139	
	HP shaft	0.056	0.066	5.43	0.020	
IP	IPC	0.154	0.286	31.98	1.69	3.61
	LPT(CMC blades&vanes)	0.091	0.329	32.95	1.92	
	LP shaft	0.011	0.021	19.88	0.01	
Fan	Fan	0.196	0.95	304.7	143.35	147.36
	Gearbox	0.053	0.181	224.65	4.00	
	Fan shaft	0.04	0.05	7.37	0.02	

Table 3 Moment inertia cases

Case1	Case2	Case3	Case4	Case5	Case6	Case7
IFan x1	IFan x 1.5	IFan x 2	IFan x 1			
IIP x1			IIP x 0.5	IIP x 1.5	IIP x 1	
IHP x1					IHP x 0.5	IHP x 1.5

2.2.2 BOV Schedule

HPC tends to choke at low power settings while IPC and Fan are likely to surge. The limited flow capacity of HPC has restricted the air mass flow in IPC and Fan where the pressure ratio is significantly boosted. Correspondingly, the last stage of IPC employs a blow-off valve to bleed the excessive flow. The main parameters involved are the blow-off air fraction (BOAF) linked to the IP shaft corrected speed (CN). The BOV bleed schedule shown in Table 4 was set as reference and implemented during the investigation of other factors. It can be seen that the emitted air is declined as the engine approaches to high power settings. When the engine accelerates from IP CN 0.55 to 1, the

BOV gradually closes with the released air fraction dropping from 13% to 0. As presented in Fig. 4, the BOAF was decreased by 10% and 30% respectively based on the reference to research the BOV influences.

Table 4 BOV schedule

IP CN	BOAF
0.55	0.13
0.7	0.1
0.8	0.06
0.9	0.03
1	0

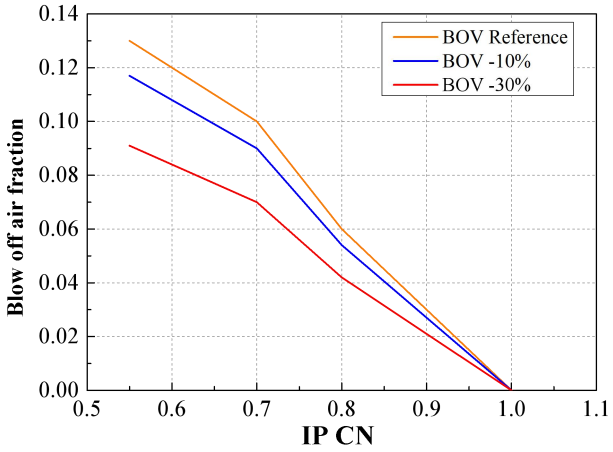

Fig. 4 BOV investigation cases.

2.2.3 Volume Packing

A further note is the volume packing, which primarily includes the mass flow difference between inlet and outlet of the same duct. During a rapid acceleration or deceleration, the mass flow of the inlet and outlet of the component would not be constant due to the mass packed in the volume. The resulted aerodynamic fluctuation would affect compressor working lines. ICV approach [12] is applied in obtaining the volume packing effects. Inter-component volume is equal to half the physical volume (PV) of the upstream and downstream components, as well as the total PV of itself. The calculated PV and ICV of each part are shown in Table 5 which also launches two additional ICV cases.

Table 5 PV and ICV and investigation case

Component	PV (m^3)	ICV x1 (m^3)	ICV x5 (m^3)	ICV x10 (m^3)
Fan	2.537	3.551	17.75	35.51
Bypass duct	2.027	3.296	16.48	32.96
IPC	0.018	1.038	5.19	10.38
HPC	0.012	0.025	0.12	0.25
Burner	0.007	0.015	0.07	0.15
HPT	0.003	0.055	0.27	0.55
LPT	0.098	0.149	0.74	1.49
Exhaust	0.100	0.148	0.74	1.48

2.2.4 PGB Heat Load

Generally, the total power losses of PGB could be categorized by non-load dependent and load-dependent power losses [6]. The former consists of seal loss, churning and windage loss from gears, the churning losses from bearings and pump powers. The latter is subdivided into bearing friction and gear mesh losses [26][27]. The gearbox efficiency map presented in Fig. 5 was employed to simplify the heat load analysis [28]. Each point on the map represents the transmission efficiency by using a blanket shaped by IP rotating speed and torque. The gearbox performance tends to be enhanced as the IP shaft has a high torque and low speed.

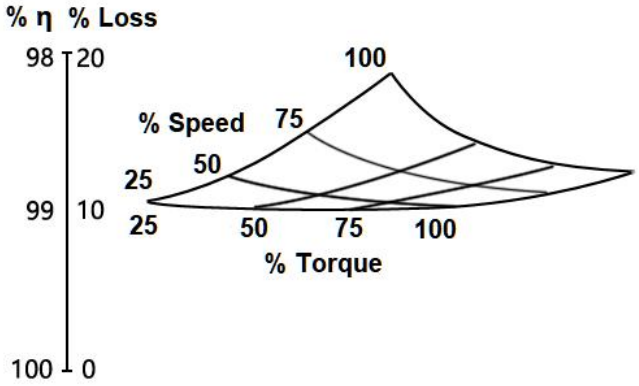

Fig. 5 Gearbox efficiency map.

However, the heat load at other segments should not be neglected, undertaking a transient simulation of the flight duty cycle would be of great necessity for the GTF engine. A 2600nm flight range mission was simulated during which the injected fuel was precisely controlled according to the thrust requirements, as shown in Fig. 6. It could be observed that the fuel flow does not remain the

same at the cruise segment but steadily declines because the onboard burned fuel relieves the aircraft weight. Block fuel is calculated using the time integrator since the PID has designated the fuel schedule for each segment. NOx is estimated by the NASA P3T3 method, as shown in Equation (2) [29].

$$EINOx = 33.2 \times (\frac{P_3}{432.7})^{0.4} \times EXP(\frac{T_3 - 459.67 - 1027.6}{349.9} + \frac{6.29 - 6.3}{53.2}) \quad (2)$$

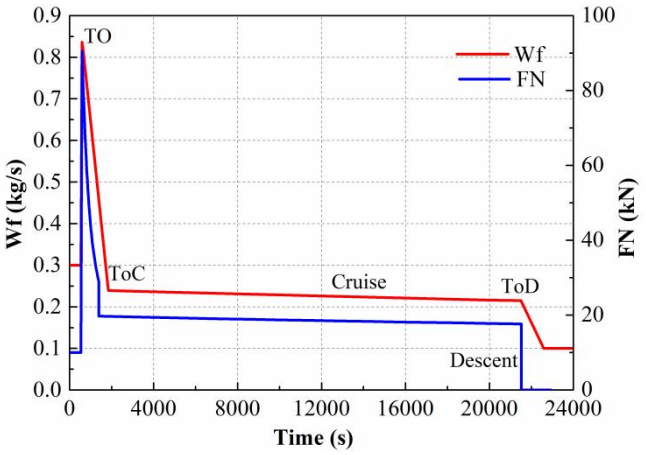

Fig. 6 Fuel schedule and thrust requirement.

3. Results and Analysis

During the transient period, compressor operating lines, surge margin (SM), net thrust, fuel flow, T4 are the most concerning parameters and were analyzed thoroughly. The gearbox power losses for different flight segments were also estimated in the flight mission assessment.

3.1 Fuel Schedule Influences

The effects of fuel schedule on HPT, IPC and Fan operating lines are illustrated in Fig. 7 and Fig. 8. As can be seen, a rapid acceleration would drive the HPC excursion nearer to the surge line. Since W4 and rotational speed could not react in such a short time, the rising fuel-air ratio leads to a higher temperature rise. Consequently, P4 shoots up to match the constant (NDMF)4. Therefore, the operating line of 4s acceleration would move closer to the surge line. Moreover, an obvious overshooting phenomenon of T4 would be induced, soaring from 1950K to 1980K, as presented in Fig. 9.

When a quick deceleration functions, the shaft delay is more prominent. The PR has to be sufficiently high to impel the airflow that has been swallowed in the engine, so the operating line

proceeds much closer to the surge line. The acceleration process shows the contrary behaviour. Regarding the Fan operating line, it behaves almost the same as IPC, as shown in Fig. 8 (b).

Fig. 9 illustrates fuel schedule influences on engine performance, including T4 and net thrust. Apparently, if the throttle lever pulls faster, T4, FN react rapidly and attain the required value in advance. For T4, the overshooting is rather significant at the end of the rapid over fueling. Thus, the fuel schedule is substantially influential in the engine transient behaviour and should be designed appropriately to ensure compressor stability. A moderate fuel schedule would be preferable for stable engine operation.

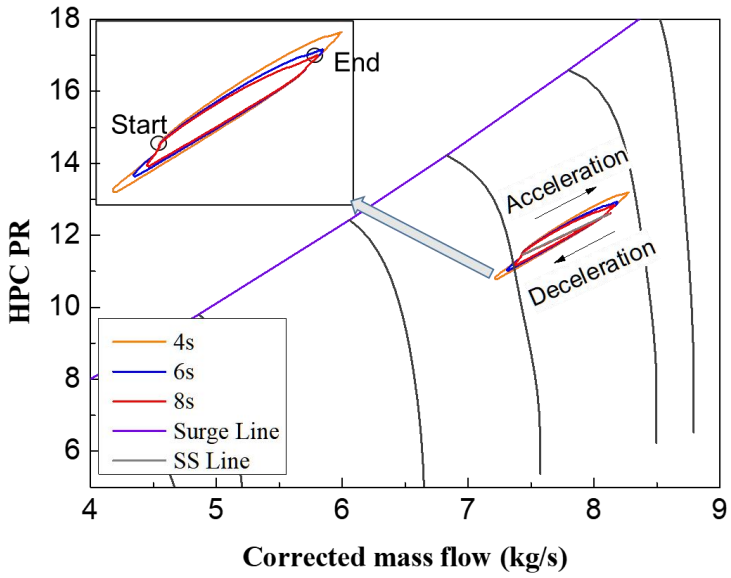

Fig. 7 HPC and IPC operating lines comparison.

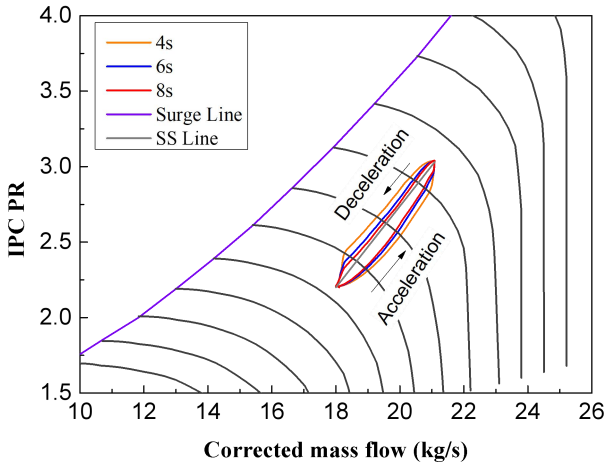

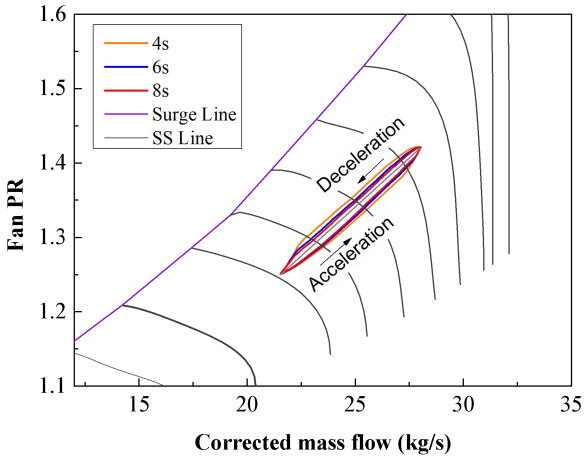

(a) IPC operating lines **(b) Fan operating lines**

Fig. 8 IPC and Fan operating lines comparison.

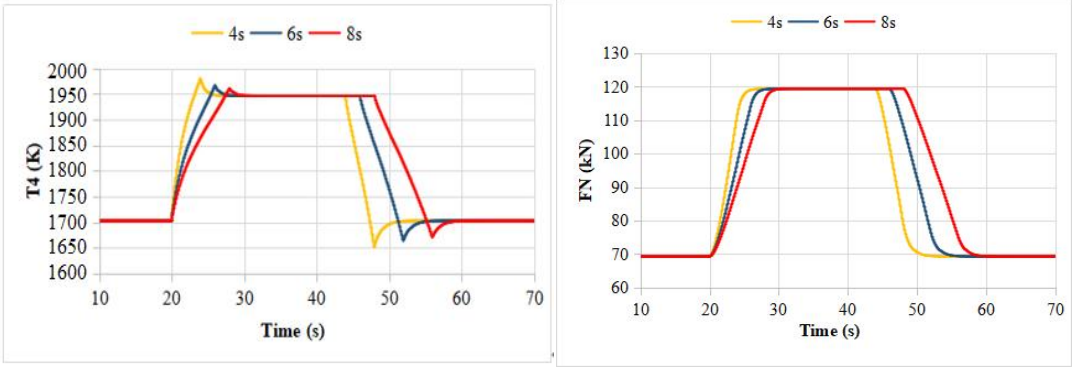

(a) T4 comparison **(b) FN comparison**

Fig. 9 T4 and FN comparison.

3.2 Shaft Inertia Influences

3.2.1 Fan Shaft Inertia

Table 3 defines three investigation cases by multiplying fan shaft inertia with 1, 1.5 and 2. Fig. 10 and Fig. 11 present the corresponding actions of the three components. It is difficult to distinguish the HPC running lines since they are very close to each other. The further excursion at the acceleration endpoint is caused by T4 overshoooting, especially for the larger inertia case. By contrast to the HPC, Fan and IPC are more sensitive to Fan shaft inertia changes and the offset of the working lines could be easily recognized.

Furthermore, the increase in Fan shaft inertia would aggravate the surge issue when the engine slows down. The reason is that the delayed shaft response curbs the decrease of the air mass flow while the PR goes up to maintain the flow capacity. The resulting performance is illustrated in Fig. 12.

It could be observed that the T4 overshooting is severer when Fan shaft inertia is doubled due to the lagged response. As expected, the thrust is reluctantly to reach the desired value for the higher inertia case.

It could be concluded that the Fan shaft inertia significantly impacts the LP system and barely disturbs the HPC. This observation highlights the effects of Fan shaft inertia, which are more profound than the fuel schedule for this specific engine. Hence, it is important to check the engine operability as well as the performance when there are some configurations changes regarding the shaft inertia.

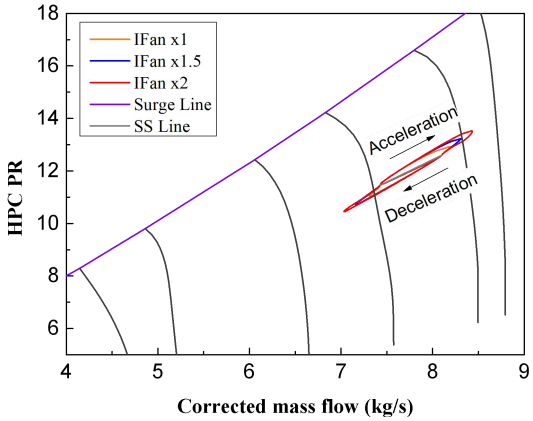

Fig. 10 HPC operating lines comparison.

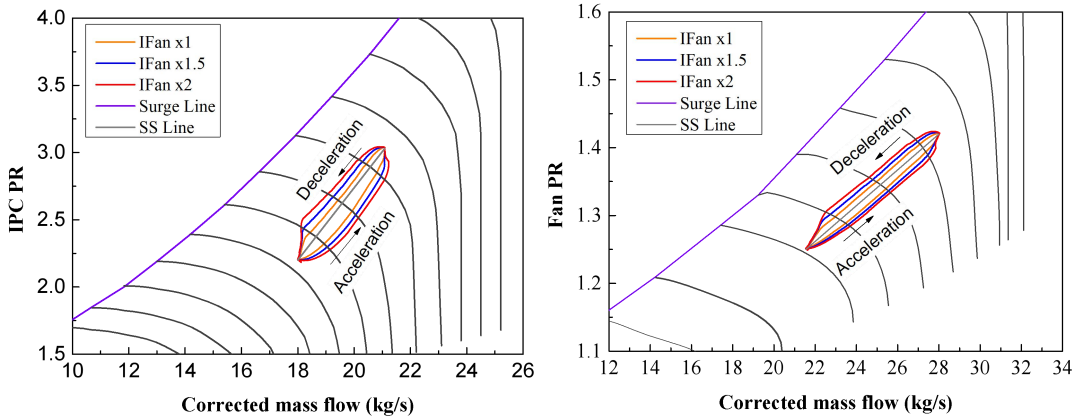

(a) IPC operating lines **(b) Fan operating lines**

Fig. 11 IPC and Fan operating lines comparison.

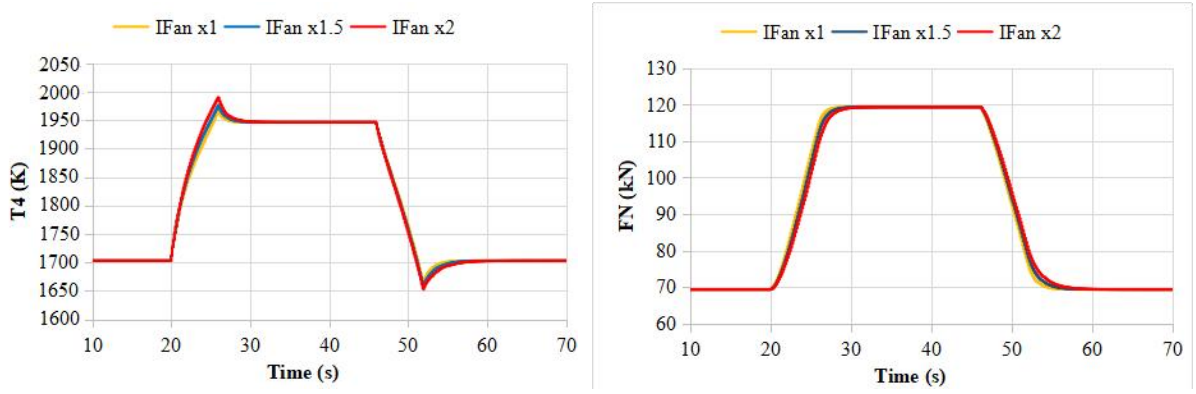

(a) T4 comparison **(b) FN comparison**

Fig. 12 T4 and FN comparison.

3.2.2 IP and HP Shaft Inertia

The three components, HPC, IPC and Fan behaved much stable as the excursions are almost overlapped even if IP shaft and HP shaft inertia are altered. Meanwhile, the corresponding T4 and thrust are also unaffected, which are not demonstrated in details. Fig. 13 depicts the related transient behaviour of the IPC caused by IP shaft and HP shaft inertia variation. The CMC application on turbines has lowered the IP shaft inertia, which more greatly deviates the two shaft inertia.

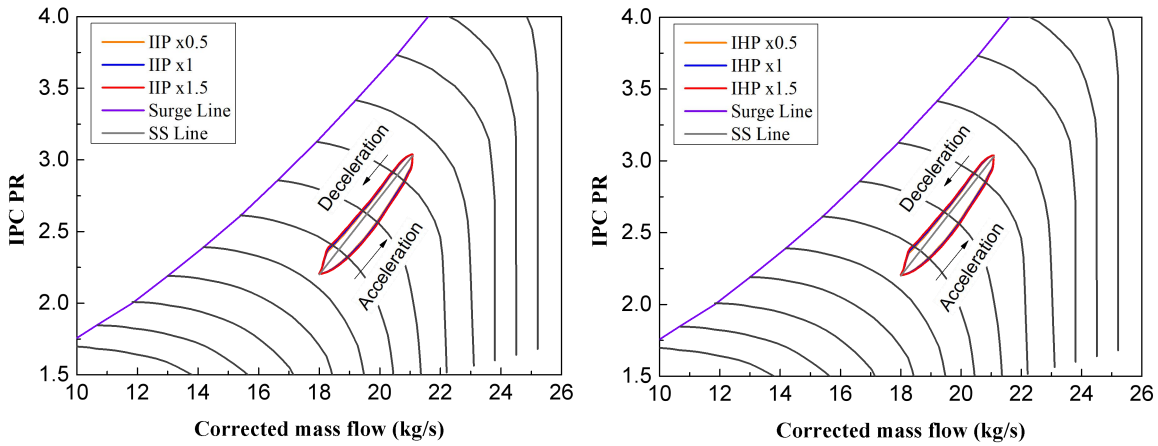

(a) IP shaft inertia influences **(b) HP shaft inertia influences**

Fig. 13 IPC operating lines comparison.

3.3 BOV Schedule Influences

The blow-off valve would release excessive air to prevent IPC and Fan surge issues and the schedule needs to be carefully designed. In this scenario, sensitivity analysis was performed by minimizing the BOAF linearly, as depicted in Fig. 4. The examined working lines of IPC and Fan impacted by the BOV schedule are demonstrated in Fig. 14. The SS lines shifted obviously and

located closer to the surge line when less air was blown off due to the fact that the weakened flow capacity drives the PR to a higher value. Whereas the engine would breathe in more air when BOV opens more widely, reducing the pressure ratio in IPC and Fan. Therefore, the operating point would be away from the surge line. Moreover, the working lines follow the same trend of running closer to the surge line during the deceleration process. IPC seems to be more vulnerable as the BOV schedule varies and tends to be unstable, especially at the low corrected speed. The lowest surge margin of IPC for each BOV schedule is 17.97%, 15.48%, 11.84% for the reference, -10% case and -30% case. The results uncovered that the released air fraction should be no more than 10% reduction on the basis of the reference schedule.

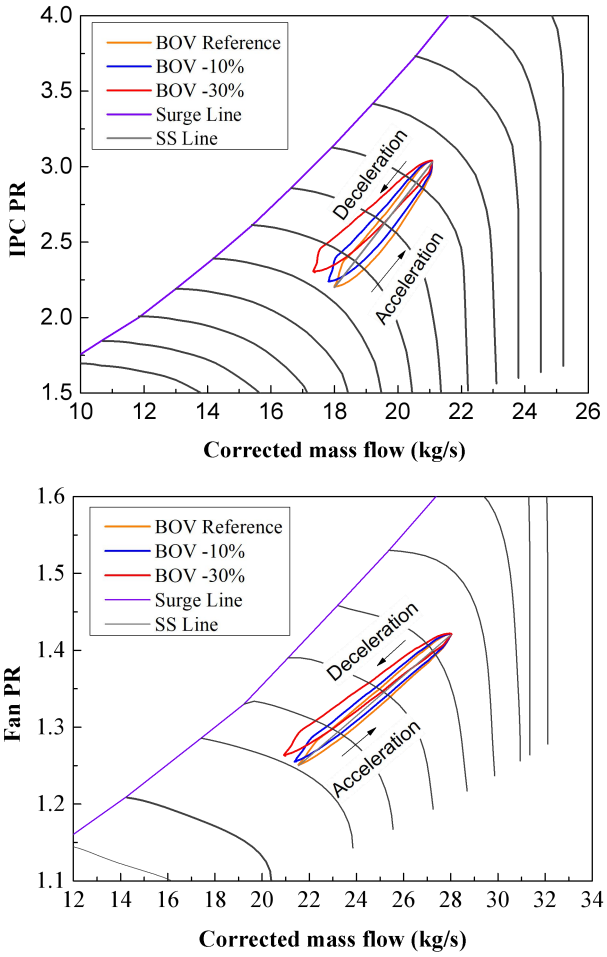

(a) IPC operating lines **(b) Fan operating lines**

Fig. 14 IPC and Fan operating lines comparison.

3.4 Volume Packing Effects

Transient behaviour could be influenced by the pressure dynamic when using the ICV approach to

carry out the simulation. The ICV was multiplied by the factor of 5 and 10, respectively, as listed in Table 5. Fig. 15 illustrates the impacts of ICV variation on HPC transient behaviour. During deceleration, the operating point of the larger volume case moves closer to the SS line. As ICV increases, more air is forced to flow out of HPC to release the pressure, resulting in more air entering into the HPT. Though T4 is decreasing, the increased HPT inlet mass flow offsets the effect of the dropped T4. Hence the HP turbine work increases and HPC PR rises.

During acceleration, the volume would store more air in HPC to increase the pressure, so HPT work reduces and HPC PR declines. On the maps of IPC and Fan, the trajectories of the ICV x10 case are on the outer border for a similar reason to that of HPC. However, the working lines of HPC, IPC and Fan in each map lay too close to each other and are not easy to identify, revealing that the Inter-component volume packing hardly affects the engine transient behaviour.

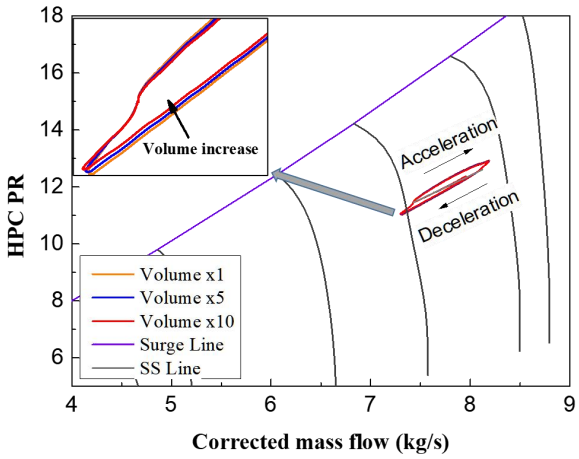

Fig. 15 HPC operating lines comparison.

3.5 Gearbox Heat Load Investigation

Gearbox heat could not be overlooked throughout the mission and may pose a critical parameter for low power rating operation. The generated heat in gearbox during engine operation could be deemed as a form of power loss. The examined results of power losses for PGB is demonstrated in Fig. 16. The blue bars mean the IP shaft input power while the red lines represent PGB power losses. Undoubtedly, take-off is the most power demanding point and followed by the climb segment, during which the gearbox would generate noticeable heat load and mechanical loss. This might inevitably affect engine performance, so it is essential to evaluate the heat load at critical flight segments.

A closer inspection on Fig. 16 shows that the power input at TO and climb are approximately 16.7MW and 14.8MW, while the losses take up about 1.10% and 1.20%. In terms of top of climb (ToC) and cruise, the losses are halved compared to those at TO and climb. Besides, the top of descent (ToD) segment produces the lowest power losses, only about 0.07MW.

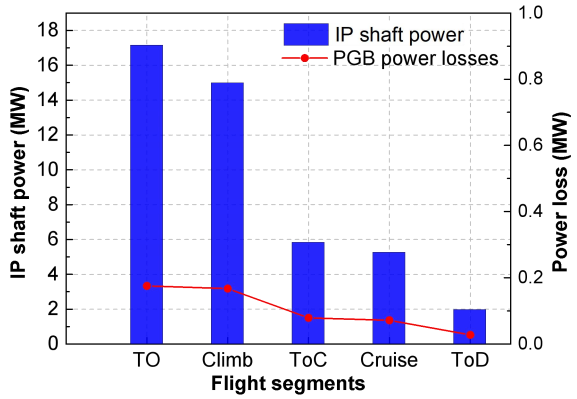

Fig. 16 Gearbox mechanical losses for each flight segment.

3.6 Inconel and CMC comparison

3.6.1 Transient Behaviour

The application of CMC material on turbine components might bring an unexpected risk of the compressor surge issue. Therefore, it is essential to explore the transient behaviour deviation of implementing CMC material from Inconel material. As can be seen from Fig. 17, the IPC map of the CMC case has been altered with the SS line and surge line moving to the left side of the Inconel case. The primary reason is the decreased core mass flow resulting from the enlarged BPR, as listed in Table 1. To be specific, the core mass flow for CMC case is lower than the Inconel since the BPR has risen from 13.15 to 15.51. Applying CMC provides extra capability for core temperature rise, which allows for a smaller core and thus all core components will be different. The maps are scaled to make sure that the peak efficiency occurs at design point. Therefore, the IPC operating lines and maps are different for the two cases. Though the two engines behave similarly during the acceleration and deceleration, the trajectory for CMC case is narrower and closer to the SS line due to the smaller shaft inertia. More importantly, the surge margin for CMC is slightly lower than the Inconel case, dropping from 15.19% to 15.05% but still satisfies the SM≥15% requirements [4]. Furthermore, the IP shaft rotary acceleration and deceleration rate of the two cases are quite different. As shown in Fig. 18,

CMC case responds faster in the first instants of the transient operating process. The fundamental cause is that the lighter rotating mass of CMC turbine generates lower inertia, which mitigates the shaft delay. One thing that should be pointed out is that the T4 overshooting is relived from 2000K to 1970K when the CMC material is applied, as shown in Fig. 19.

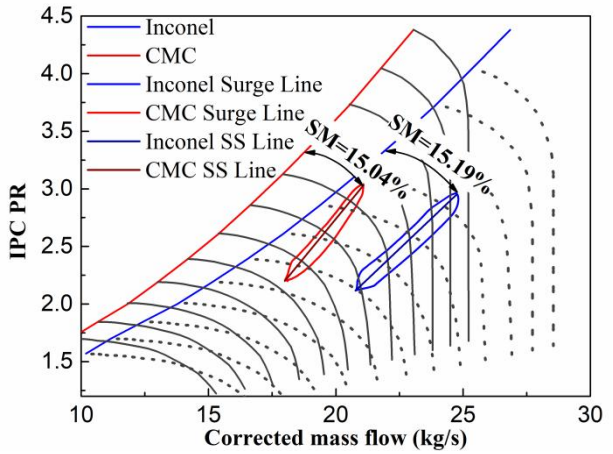

Fig. 17 Inconel and CMC IPC operating line comparison.

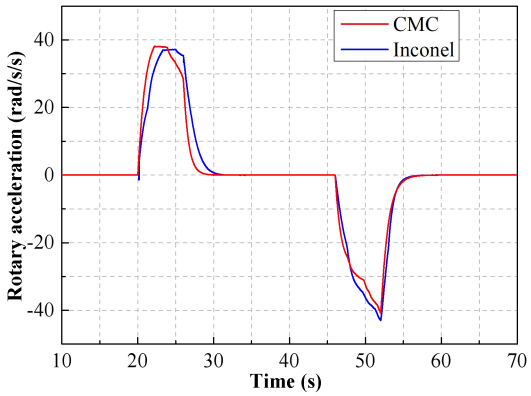

Fig. 18 Inconel and CMC IP shaft rotary acceleration comparison.

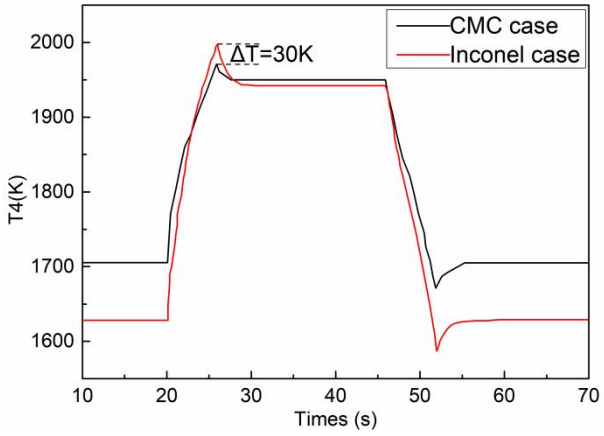

Fig. 19 Inconel and CMC T4 comparison.

3.6.2 Flight Mission Performance

The 2600nm flight mission assessment on block fuel and emissions was performed in Amesim to study the benefits of utilizing CMC material for civil aircraft. In Fig. 20, there is a clear drop in block fuel, NOx, noise, CO2 and H2O, falling by 4.9%, 5.9%, 1.0%, 4.9% and 4.9% respectively. The improvement mainly comes from the reduction in SFC and engine weight, approximate 3.8% and 2.8% according to Reference [22]. It should be noted that the block fuel reduction resulting from SFC decrease and engine weight drop is 4.54% and 0.38% respectively. It highlights the importance of lowering the SFC to obtain a better fuel economy. The 4.9% saved block fuel would help the airliners cut 0.08 million dollars fuel cost per year, providing the fuel price is 1.567 USD/gallon [30]. Undoubtedly, CMC turns out to be a promising material that would significantly boost engine performance and reduce pollution.

Moving on to consider the heat load difference during the flight mission for the two cases. What striking out in Fig. 21 is that the CMC case emits greater heat rejection for all the critical segments, such as 3.98% and 6.59% increase at take-off and climb. The heat rejection is closely related to the gearbox efficiency which is determined by the transmitted torque. The smaller shaft inertia of CMC case offers low torque and thus formulates an inferior transmission efficiency. Therefore, the fuel oil system might not be capable of addressing the increased heat load of CMC engine. Hence, the thermal management system would need a redesign to reinforce the superb performance of the geared turbofan engine employing CMC turbines.

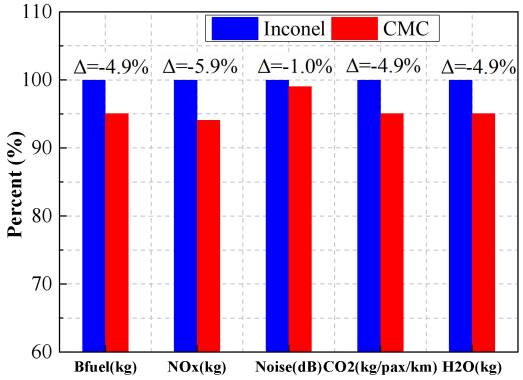

Fig. 20 Block fuel and emissions comparison.

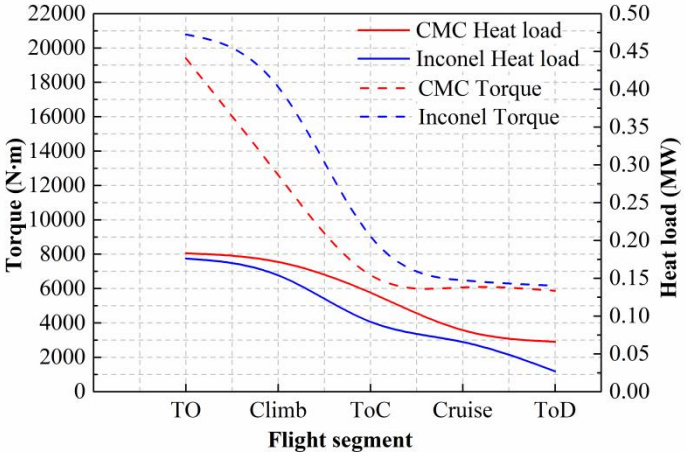

Fig. 21 Heat load comparison.

4. Conclusions

This paper performs a systematic investigation on the transient behaviour of the geared turbofan engine implementing CMC materials. Sensitivity analysis regarding the fuel schedule, shaft inertia, BOV profile and volume packing were conducted. Afterwards, the comparisons between CMC case and Inconel case were carried out including flight mission performance and PGB heat load, to reveal the advantages of using CMC. The observations could be concluded as below:

1. CMC engine acts differently from the Inconel engine in terms of the excursion, surge margin, rotary acceleration rate, and T4 overshooting. The IPC surge margin has a 0.15% drop but still is free from surge. The decreased shaft inertia allows a prompt response following a sudden throttle manoeuvre. Besides, it shows a significant advantage in relieving the overshooting phenomenon with the maximum T4 levelling off 30K. In the long-term consideration, it would significantly prolong the engine lifespan and cut the maintenance expense.

2. The running lines formed by operation points alleviates from the SS lines during transient operations. The Fan shaft inertia was identified to be the most influential factor that impacts the transient behaviour. Secondly, slam deceleration should be avoided to maintain the operability of IPC and Fan. Thirdly, BOAF at low corrected speed should be sufficient enough to ensure compressor stability and a maximum allowable reduction in BOAF is 10% compared to the reference. Finally, the volume packing effects could be ignored and would not push the key components to risk circumstances.

3. Gearbox heat load is nonnegligible during the whole flight mission and may trigger a thermal management problem at low power settings. Additionally, CMC implementation on the turbine would generate extra heat load, about 3.98% rise at take-off, for its lighter density and lower shaft inertia. The take-off and climb segments produce the largest power losses and take up about 1.1% of the IP shaft input power, indicating a significant cooling requirement in the power gearbox. The fuel oil system would expect a design modification to soak the increased heat rejection.

4. For an aircraft level assessment, the CMC engine has witnessed a boost both in the aspects of economy and environment. A 4.9% block fuel reduction could attain 0.08 million dollars in annual fuel cost saving. Moreover, it could also provide 5.9% and 1.0% decline in NOx and noise. Finally, 4.9% drop in CO2 per passenger kilometre could be achieved by adopting the CMC turbine components.

Acknowledgments

The authors would like to thank AECC Shenyang Engine Research Institute for the support and fund.

References

[1]. Dewanji, D., Rao, G. A. and Van Buijtenen, J. (2009). Feasibility study of some novel c oncepts for high bypass ratio turbofan engines, Proceedings of the ASME Turbo Expo, 1 (0), pp. 51–61. https://doi.org/10.1115/GT2009-59166.

[2]. Larsson, L., Avell, R. and Gronstedt, T. (2011). Mission Optimization of the Geared Turb ofan Engine, ISABE-2011-1314, pp. 1-7.

[3]. Saravanamuttoo H.I.H., Rogers G.F.C., Cohen H., et al. (2017). Gas turbine theory, Seven th edition. Pearson Education Limited, Great Britain, 2017.

[4]. Walsh, P. and Fletcher, P. (2004), Gas Turbine Performance, 2nd edition, Blackwell Scien ce Ltd, Great Britain, 2004.

[5]. Sexton, W. R., (2001), A Method to Control Turbofan Engine Starting by Varying Compr essor Surge Valve Bleed, MSc Thesis, Faculty of the Virginia Polytechnic Institute and St ate University, 2001.

[6]. Mourouzidis C. (2016). Cycle optimization & preliminary design of very low specific thr ust turbofan engines. PhD thesis, Cranfield University, 2016.

[7]. Woodward, R. P., Hughes, C. E., & Podboy, G. G. (2006). Fan Noise Reduction with In creased Bypass Nozzle Area. Journal of Aircraft, 43(6), 1719–1725. doi:10.2514/1.19359.

[8]. Halliwell, I., Justice, K. (2012). Fuel Burn Benefits of a Variable-Pitch Geared Fan Engin e. 48th AIAA/ASME/SAE/ASEE Joint Propulsion Conference & Exhibit. doi:10.2514/6.20 12-3912.

[9]. Miguel Angel V.A. (2015). Preliminary design and optimisation of a power gearbox for t he ULTRAFANTM geared engine. MSc Thesis. Cranfield University, 2015.

[10].Ortiz, J (2014). Estimation of Weight and Power Losses of a Reduction System for a Ge ared Turbofan Engine. MSc Thesis, Cranfield University, 2014.

[11].Manuel O, Bernd S, Balazs M. (2019). Efficiency of worm gear drives under transient o perating conditions, Journal of Tribology, Volume 141, Issue 12, 2019. https://doi.org/10.11 15/1.4044655.

[12].Wang Q. (2016). Gas turbine performance simulation of transient operation. MSc thesis, Cranfield University, 2016.

[13].Zhang W. (2015). Engine modelling and control system design for a geared turbofan. MS c thesis, Cranfield University, 2015.

[14].Roumeliotis I., Theoklis N, Broca O., etc al. (2018). Dynamic simulation of a rotorcraft hybrid engine in Simcenter Amesim, Proceedings of the 44th European Rotorcraft Forum (ERF2018), pp.1-14.

[15].Yang Q. (2015). Transient performance simulation and control law design of a turboshaft

engine, MSc thesis, Cranfield University, 2015.

[16].L. P. Zawada, G. Y. Richardson, G. Doppes, and P. C. Spriet. CMCs for aerospace turbine engine exhaust nozzles. Proceedings of the 5th International Conference on High Temperature Ceramic Matrix Composites, HT-CMC5, conference, Seattle, WA, September 12−16, 2004.

[17].J. M. Staehler and L. P. Zawada. Performance of four ceramic-matrix composite divergent flap inserts following ground testing on an F110 turbofan engine. J. Am. Ceram. Soc., 83(7), 1727−1738 (2000).

[18].L. Zawada, E. Bouillon, G. Ojard, G. Habarou, C. Louchet, D. Feindel, P. Spriet, C. Logan, T. Arnold, K. Rogers, et al. Manufacturing and flight test experience of ceramic matrix composites seals and flaps for the F100 gas turbine engine. ASME Paper No. GT2006 - 90448 (2006).

[19].J. A. DiCarlo and M. van Roode. CMC developments for gas turbine engine hot section components. ASME Paper No. GT2006- 90151 (2006).

[20].V. Vedula, J. Shi, D. Jarmon, S. Ochs, L. Oni, T. Lawton, K. Green, L. Prill, J. Schaff, G. Linsey, et al. CMC turbine vanes for gas turbine engines. ASME Paper No. GT2005-68229 (2005).

[21].Langenbrunner, N., Weaver, M., Dunn, M. G., Padova, C., & Barton, J. (2014). Dynamic Response of a Metal and a CMC Turbine Blade During a Controlled Rub Event Using a Segmented Shroud. Journal of Engineering for Gas Turbines and Power, 137(6), 062504. doi:10.1115/1.4028685

[22].Mo D (2021). Conceptual design of a two-shaft high bypass turbofan engine for entry-into-service 2025, MSc thesis, Cranfield University, 2021.

[23].Siemens, Simcenter Amesim User Manual, 2020.

[24].Joseph E. Grady. (2013). CMC technology advancements for gas turbine engine applications. American Ceramic Society's 10th Pacific Rim Conference on Ceramic and Glass Technology, 2013, San Diego, CA.

[25].Motion Analysis. (2006). Available at: http://files.engineering.com/download.aspx?folder=96ad1dc6-a47f-4332-91bc-5e96a02aaf1c&file=Calculating_and_Using_Moments_of_Inertia.pdf.

[26].American National Standard (2006). Design Manual for Enclosed Epicyclic Gear Drives, 2006.

[27].ISO 14179-1:2001. Gears-Thermal Capacity-Part 1: Rating gear drives with thermal equilibrium at 95º C sum temperature.

[28].Dominy J. (1987). Transmission efficiency in advanced aerospace powerplant, Rolls-Royce Plc. AIAA/SAE/ASME/ASEE 23rd Joint Propulsion Conference. San Diego. California, 1987. AIAA-87-2043. https://doi.org/10.2514/6.1987-2043.

[29].Daggett, D. L. (2004). Water misting and injection of commercial aircraft engines to reduce airport NOx, NASA/CR-2004-212957, C&EA–BQ130–Y04–002, 2004.

[30].Hensey R, Magdalina A. (2018). A320 NEO vs. CEO comparison study. FPG Amentum. pp. 1-15.

Nomenclature

BPR	bypass ratio
BOV	blow-off valve
CR	cruise
ICV	intercomponent volume
IFAN	fan shaft inertia
IHP	high pressure shaft inertia
IIP	low pressure shaft inertia
J	moment inertia
mR	rotating mass
ND	non-dimensional mass flow
PGB	power gearbox
PR	pressure ratio
PV	physical volume
RO	outer radius
Ri	inner radius
SM	surge margin
SS	steady state
T	torque
TO	take-off
ToC	top of climb
VAN	variable area nozzle
VIGV	variable inlet guide vane
VPF	variable pitch fan
VSV	variable stator valve

2022-12-16

Dynamic simulation and aircraft level assessment of CMC implementation on GTF engine

Mo, Da

Springer

Mo D, Roumeliotis I, Liu Y, et al., (2023) Dynamic simulation and aircraft level assessment of CMC implementation on GTF engine, International Journal of Aeronautical and Space Sciences, Volume 24, Issue 3, July 2023, pp. 812-823

https://doi.org/10.1007/s42405-022-00559-z